



UNIVERSITY
OF TRENTO

DEPARTMENT OF INFORMATION AND COMMUNICATION TECHNOLOGY

38050 Povo – Trento (Italy), Via Sommarive 14
<http://www.dit.unitn.it>

DESIGN OF A PRE-FRACTAL MONOPOLAR ANTENNA FOR 3.4-3.6 GHz
WI-MAX BAND PORTABLE DEVICES

R. Azaro, G. Boato, M. Donelli, A. Massa, and E. Zeni

August 2005

Technical Report DIT-05-057

Design of a Pre-Fractal Monopolar Antenna for 3.4 - 3.6 GHz Wi-Max Band Portable Devices

Renzo Azaro, *IEEE Member*, Giulia Boato, Massimo Donelli, Andrea Massa, *IEEE Member*, Edoardo Zeni.

DEPARTMENT OF INFORMATION AND COMMUNICATION TECHNOLOGY

University of Trento, Via Sommarive 14, 38050 Trento, ITALY

Tel.: +39 0461 882057, Fax: +39 0461 882093

E-mail: andrea.massa@ing.unitn.it,

{[renzo.azaro](mailto:renzo.azaro@ing.unitn.it), [massimo.donelli](mailto:massimo.donelli@ing.unitn.it), [giulia.boato](mailto:giulia.boato@ing.unitn.it)}@dit.unitn.it

Web: <http://www.eledia.ing.unitn.it>

Design of a Pre-Fractal Monopolar Antenna for 3.4 - 3.6 GHz Wi-Max Band Portable Devices

Renzo Azaro, *IEEE Member*, Giulia Boato, Massimo Donelli, Andrea Massa, *IEEE Member*, Edoardo Zeni.

Abstract - In this letter, the design of a miniaturized monopolar pre-fractal antenna for the 3.4 – 3.6 GHz Wi-Max band is presented. The geometrical configuration of the monopolar antenna, printed on a planar dielectric substratum, has been synthesized by means of a Particle Swarm Optimizer in order to minimize the linear dimensions of the device and to obtain Voltage Standing Wave Ratio values within specifications. The results of numerical simulations are shown and compared, in terms of VSWR, with the experimental measurements.

Key Words: Wireless Systems, Antennas Design, Fractal Antennas, Microstrip antennas, Particle Swarm Optimizer, Wi-Max Portable Devices.

1. INTRODUCTION

The growing demand of wireless services requires the definition of new standards able to provide an increased degree of mobility for the end-user and a higher speed of data transmission. Among emerging standards, one of the most promising is the *IEEE 802.16 Wireless Metropolitan Area Network Air Interface* (generally called *WiMax*) able to support high-speed wireless broadband applications with rather long reach, mobility, and roaming. More in detail, WiMax is a standard for fixed broadband wireless access systems, which employ a point-to-multipoint architecture and operate between 10 and 66 GHz providing only Line-Of-Sight (LOS) applications.

In order to extend the 802.16 Air Interface standard guaranteeing Non-Line-Of-Sight (NLOS) features, a successive release called *IEEE 802.16a* has been proposed to deliver services over a scalable, long range, high capacity wireless communications for carriers and service providers around the world. It covers the frequency range between 2 and 11 GHz and it is suitable for last-mile applications. In such a framework, the available band between 3.4 – 3.6 GHz turns out to be of particular interest since it doesn't require a LOS propagation and can be usefully exploited for end-user wireless portable devices.

As far as wireless portable devices are concerned, it is mandatory to develop miniaturized radiators able to guarantee a good efficiency and reliability. In such a field, fractal antennas seem to be good candidates for achieving reduced dimensions keeping suitable radiation properties. As a matter of fact, the use of fractal geometries (or more precisely, pre-fractal geometries that are built with a finite number of fractal iterations) for antenna synthesis has been proven to be very useful in order to achieve miniaturization and enhanced bandwidth [1][2]. Recently, some interesting applications have been presented in literature [3][4][5].

This letter presents the optimized synthesis of a pre-fractal Koch-like antenna printed on a dielectric substratum operating in the 3.4 – 3.6 WiMAX band. The optimization of the fractal geometry is carried out through a numerical procedure based on a particle swarm optimizer (PSO) [6][7][8]. In order to assess the effectiveness of the design procedure and of the arising features of the optimized antenna, the numerical results are compared

with the measurements from an experimental prototype as well as with the data concerned with standard structures.

2. WiMAX ANTENNA DESIGN

The design of the Wi-Max antenna has been formulated as an optimization problem fixing suitable constraints in terms of impedance matching at the input port (VSWR values) in the 3.4 – 3.6 GHz frequency band and in terms of size reduction compared to the length of a standard quarter-wave monopole antenna. As far as an antenna for portable devices is concerned, the radiation characteristics of a monopolar quarter-wave-like pattern have been assumed. Because of the broad frequency band required by 802.16 WiMAX applications, the antenna is required to present a Voltage Standing Wave Ratio lower than $VSWR_{\max} = 1.8$ in the 3.4 – 3.6 GHz frequency range, which results in a reflected power at the input port lower than 10% of the incident power. From a geometrical point of view, a size reduction of more than 20 % compared to a standard quarter-wave resonant monopole is required. Moreover, the antenna is also required to belong to a physical platform of dimensions $L_{\max} = 16$ [mm] \times $H_{\max} = 10$ [mm].

By considering a microstrip structure printed on a planar dielectric substratum, the parameters to be optimized are the fractal geometry and the widths and lengths of each fractal segment. As far as the general shape of the generating antenna is concerned, the trapezoidal curve proposed in [5] has been used. Therefore, the antenna structure is uniquely determined by the following parameters: $s_1, s_2, s_4, s_5, \theta_2, \theta_4$ (i.e., the parameters that define the set of affine transformations employed by the iterated function system (IFS) [5] for generating pre-fractal antenna elements), L (i.e., the projected length of the fractal structure), and w_1, w_2, w_3, w_4, w_5 (i.e., the widths of the fractal segments).

In order to satisfy the project guidelines determining the array $\underline{\gamma} = \{s_1, s_2, s_4, s_5, \theta_2, \theta_4; w_i, i = 1, \dots, 5\}$, the following cost function, defined as the least-square difference between requirements and estimated specifications, has been optimized:

$$F(\underline{\gamma}) = \sum_{i=0}^{I-1} \left\{ \max \left[0, \frac{\Psi\{i\Delta f\} - VSWR_{\max}}{VSWR_{\max}} \right] \right\} \quad (1)$$

where Δf is the sampling frequency interval in the 3.4 – 3.6 GHz frequency band and $\Psi\{i\Delta f\} = \Psi(\underline{\gamma})$ is the VSWR value at the frequency $f = i\Delta f$ when the antenna structure defined by the array $\underline{\gamma}$ is considered. Furthermore, in order to avoid the generation of impractical solutions (due to their intricate and convoluted shapes) some physical constraints have been defined on the antenna parameters and a penalty has been imposed on those configurations that while not unfeasible would be difficult to realize (e.g., higher fractal orders or large ratio between width and length of the fractal segment).

To minimize (1) and according to the guidelines given in [7], a suitable implementation of the PSO [9] has been used in conjunction with an IFS generating software and a method-of-moments (MoM) simulator [10]. Starting from each of the trial arrays $\underline{\gamma}_m^{(k)}$ (m being the trial array index, $m = 1, \dots, M$; k being the iteration index, $k = 1, \dots, K$) defined by the PSO, the IFS generates the corresponding pre-fractal antenna structure. The corresponding VSWR value is computed by means of the MoM simulator, which takes into account the presence of the dielectric slab and of the reference ground plane assumed of infinite extent. The iterative process continues until $k = K$ or $\Omega_{opt} \leq \eta$, η being the convergence threshold and $F^{opt} = \min_{k,m} \{F[\underline{\gamma}_m^{(k)}]\}$.

3. NUMERICAL AND EXPERIMENTAL VALIDATION

The specific PSO adopted in this work considers a population formed by $M = 15$ trial solutions, a threshold $\eta = 10^{-3}$, and a maximum number of iterations equal to $K = 500$. The remaining parameters of the PSO have been set, according to the reference literature [7], as in [9].

As an illustrative example of the optimization process, Fig. 1 shows the evolution of the geometry of the antenna structure during the iterative process. At each iteration, the structure of the best solution (i.e., $\underline{\gamma}_{opt}^{(k)} = \arg(\min_m \{F[\underline{\gamma}_m^{(k)}]\})$) is given and the plot of the

corresponding VSWR function is reported in Fig. 2. As it can be observed, starting from a completely mismatched behavior corresponding to the structure shown in Fig. 1.(a) ($k = 0$), the solution improves until to the final shape [Fig. 1.(e) - $k = k_{conv}$] that fits the requested specification in terms of both VSWR [Fig. 2] and overall dimensions. As a matter of fact, the synthesized structure satisfies the geometrical requirements since its transversal and longitudinal dimensions are respectively equal to $L_{opt} = 13.39$ [mm] along the x -axis and $H_{opt} = 5.42$ [mm] along the y -axis. In particular, the projected length L_{opt} turns out to be lower than that of the resonant monopole printed on FR4 substratum, with a reduction equal to 24.77 %.

Concerning the computational complexity of the optimization procedure, Figure 3 shows the plot of the cost function versus the iteration number. Both the optimal cost function value $F_{(k)}^{opt} = \min_m \{F[\underline{\gamma}_m^{(k)}]\}$ and the average value $av\{F_{(k)}\} = \frac{1}{M} \sum_{m=1}^M F[\underline{\gamma}_m^{(k)}]$ are reported. The optimization required approximately $k_{opt} = 270$ iterations, with a CPU-time for each iteration of about 0.5 sec.

Because of the satisfactory numerical results, an experimental validation has been carried out. The antenna prototype has been built by using a photolithographic printing circuit technology following the geometric guidelines of the optimized geometry shown in Fig. 1(e). For the VSWR measurements, the antenna prototype (Fig. 4) has been equipped with a SMA connector and it has been placed on a reference ground plane with dimensions equal to 90 [cm] \times 140 [cm]. The VSWR has been measured with a scalar network analyzer placing the antenna inside an anechoic chamber.

Computed and measured VSWR values have been compared and the results are shown in Figure 5. As it can be noticed, measured as well as simulated VSWR values satisfy the project's specifications in the 3.4 – 3.6 GHz band. Even though a reasonable agreement between the simulation and the experimental results can be observed, some differences occur and the VSWR values measured in the WiMax band turn out to be greater than those simulated. Such a behavior can be attributed to the approximations

introduced in the numerical simulator for modeling the dielectric properties of the FR4 substratum and the ground plane.

For comparison purposes, the VSWR values of the pre-fractal antenna are also compared with those of a resonant quarter wave monopole ($L_{\lambda/4} = 7.8$ [mm] long printed on a FR4 substratum – called “*resonant monopole*”) and a straight monopole with the same length L_{opt} of the WiMAX antenna (called “*short monopole*”). As expected, the short monopole is not able to fit the VSWR specifications in the requested band. On the other hand, the simulated values of the resonant monopole seem to indicate some difficulties in satisfying the VSWR constraint at the extremes of the frequency range and they shown a small margin at the central frequency, as well.

Finally, for completeness, the same comparative assessment has been also carried out in terms of gain functions along the horizontal and vertical planes (Fig. 7). More in detail, Figure 7(a) plots the differences in the horizontal plane between the gain function of the WiMAX antenna and that of the resonant monopole and of the short monopole, respectively. The same quantities are also shown in Fig. 7(b) where the vertical gain functions are analyzed. As expected, the radiation properties of the optimized WiMAX fractal antenna are very close to those of a conventional monopole as requested for a portable wireless device.

4. CONCLUSIONS

The design and optimization of a pre-fractal WiMAX band antenna printed on dielectric substratum has been described. The antenna structure has been synthesized through a suitable particle swarm algorithm by optimizing the parameters of a Kock-like pre-fractal geometry in order to comply with the geometrical requirements as well as the impedance matching constraints in the 3.4 – 3.6 GHz band. A prototype of the WiMAX antenna has been built and some comparisons between measured and simulated VSWR values have been carried out in order to assess the effectiveness of the resulting antenna and of the overall design procedure.

ACKNOWLEDGMENTS

This work has been partially supported by the *Center of REsearch And Telecommunication Experimentations for NETworked communities* (CREATE-NET).

REFERENCES

- [1] D. H. Werner and R. Mittra, *Frontiers in electromagnetics*. Piscataway: IEEE Press, 2000.
- [2] J. Gianvittorio and Y. Rahmat-Samii, “Fractals antennas: A novel antenna miniaturization technique, and applications,” *IEEE Antennas Propagat. Mag.*, vol. 44, pp. 20–36, Feb. 2002.
- [3] C. P. Baliarda, J. Romeu, and A. Cardama, “The Koch monopole: A small fractal antenna,” *IEEE Antennas Propagat. Mag.*, vol. 48, pp. 1773–1781, Nov. 2000.
- [4] S. R. Best, “On the performance properties of the Koch fractal and other bent wire monopoles,” *IEEE Trans. Antennas Propagat.*, vol. 51, pp. 1292–1300, Jun. 2003.
- [5] D. H. Werner, P. L. Werner, and K. H. Church, “Genetically engineered multiband fractal antennas,” *Electron. Lett.*, vol. 37, pp. 1150–1151, Sep. 2001.
- [6] J. Kennedy, R. C. Eberhart, and Y. Shi, *Swarm Intelligence*. San Francisco: Morgan Kaufmann Publishers, 2001.
- [7] J. Robinson and Y. Rahmat-Samii, “Particle swarm optimization in electromagnetics,” *IEEE Trans. Antennas Propagat.*, vol. 52, pp. 397–407, Feb. 2004.
- [8] M. Donelli and A. Massa, “A computational approach based on a particle swarm optimizer for microwave imaging of two-dimensional dielectric scatterers,” *IEEE Trans. Microwave Theory Techn.*, vol. 53, pp. 1761-1776, May 2005.
- [9] R. Azaro, F. De Natale, M. Donelli, A. Massa, and E. Zeni, “Optimized design of a multi-function/multi-band antenna for automotive rescue systems,” *IEEE Trans. Antennas Propagat.* - Special Issue on “*Multifunction Antennas and Antenna Systems*,” in press.
- [10] R. F. Harrington, *Field Computation by Moment Methods*. Malabar, Florida: Robert E. Krieger Publishing Co., 1987.

FIGURE CAPTIONS

Figure 1. Geometry of the fractal WiMAX monopole at different iteration steps of the optimization procedure: (a) $k = 0$, (b) $k = 10$, (c) $k = 50$, (d) $k = 100$, and (e) $k = k_{opt}$.

Figure 2. Simulated VSWR values at the input port of the fractal monopole antenna at different iteration steps of the optimization procedure.

Figure 3. Behavior of the cost function versus the iteration number.

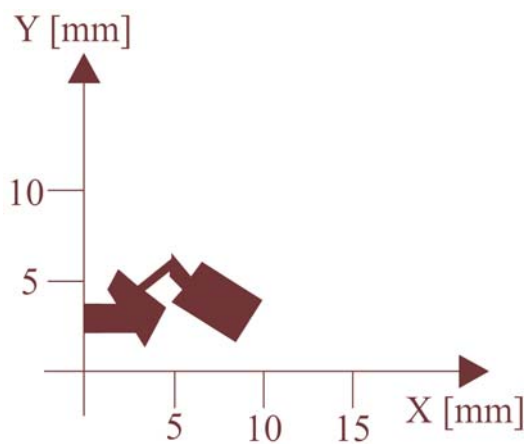
Figure 4. Photograph of the prototype of the pre-fractal monopolar WiMAX.

Figure 5 WiMAX pre-fractal antenna: comparison between measured and simulated VSWR values.

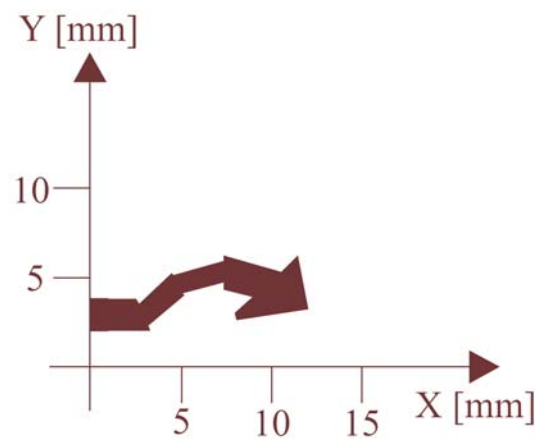
- - - - - Requirements
 - - - - - WiMAX Measured Data
 _____ WiMAX Simulated Data
 - - - - - Resonant monopole simulated data
 - - - - - Short monopole simulated data

Figure 6. WiMAX band fractal antenna gain functions: (a) difference in the horizontal plane between the gain function of the WiMAX antenna and that of the resonant monopole, and between WiMAX and short monopole; (b) difference in the vertical plane between the gain function of the WiMAX antenna and that of the resonant monopole, and between WiMAX and short monopole.

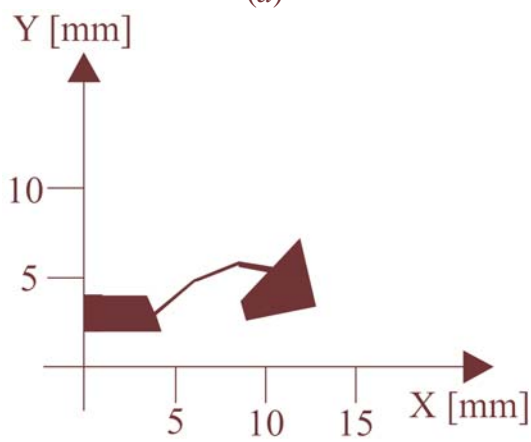
_____ WiMAX vs quarter wave resonant monopole
 _____ WiMAX vs short monopole



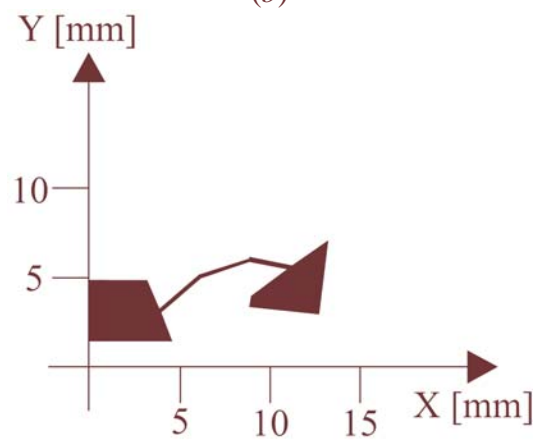
(a)



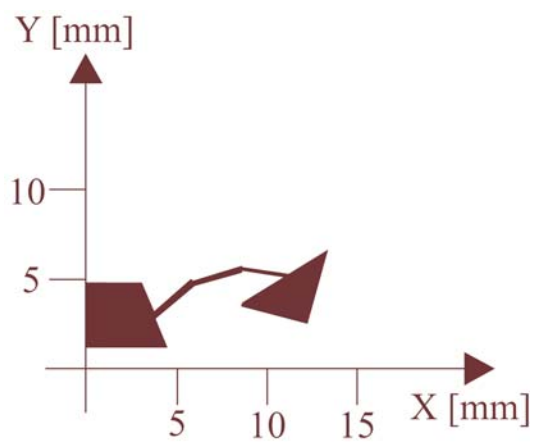
(b)



(c)



(d)



(e)

Fig. 1 – R.Azaro et al., “Design of a pre-fractal monopolar antenna”

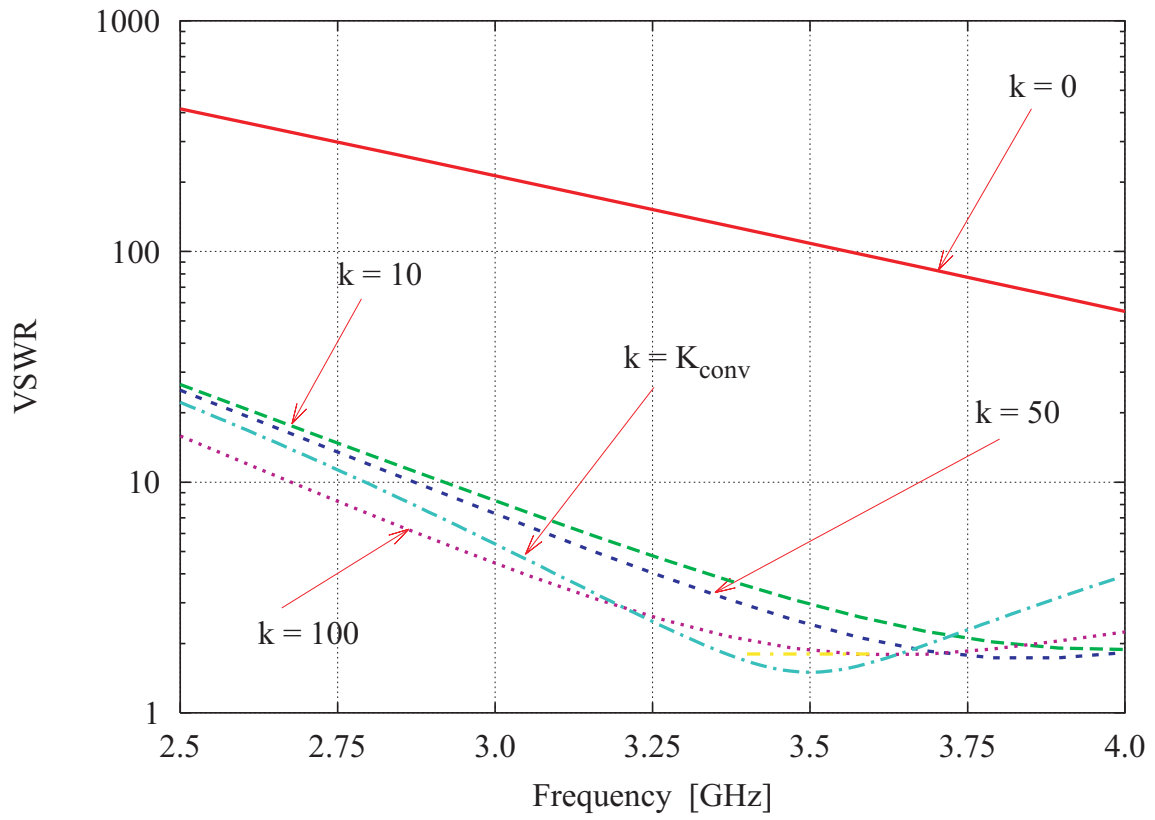


Fig. 2 – R.Azaro et al., “Design of a pre-fractal monopolar antenna ...”

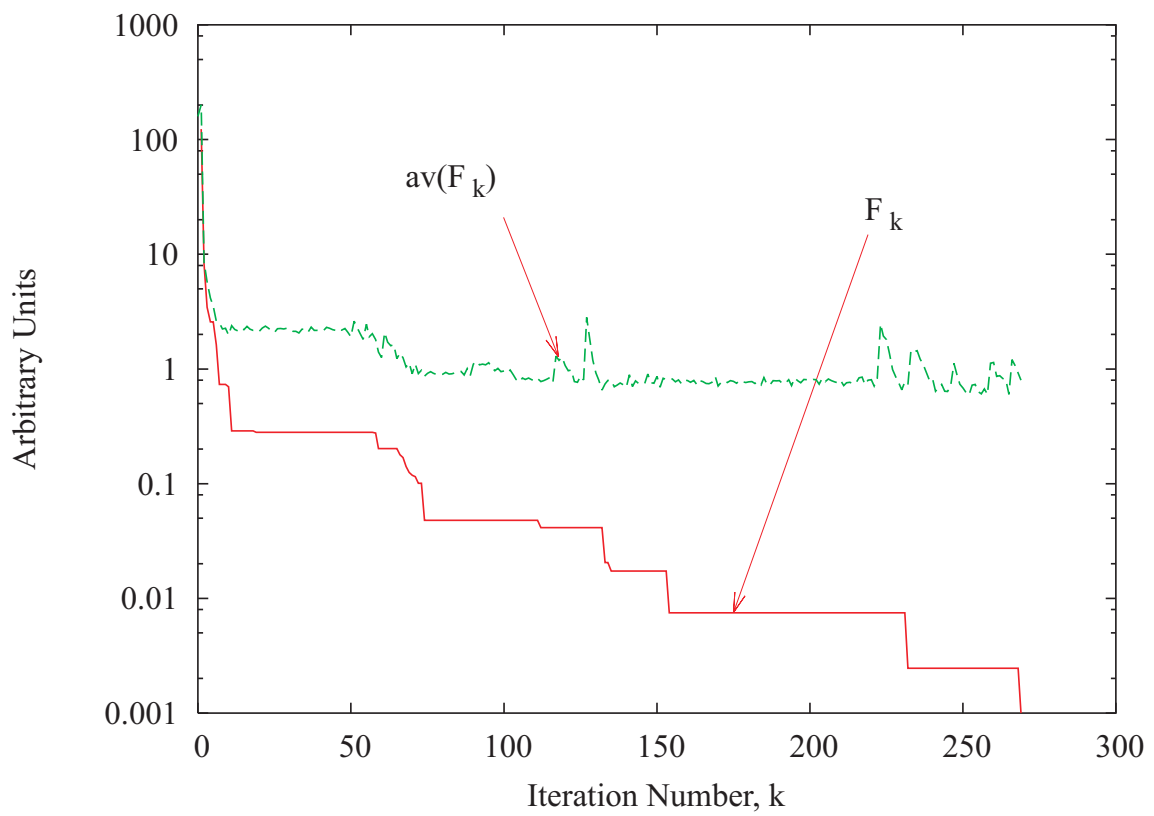


Fig. 3 – R.Azaro et al., “Design of a pre-fractal monopolar antenna”

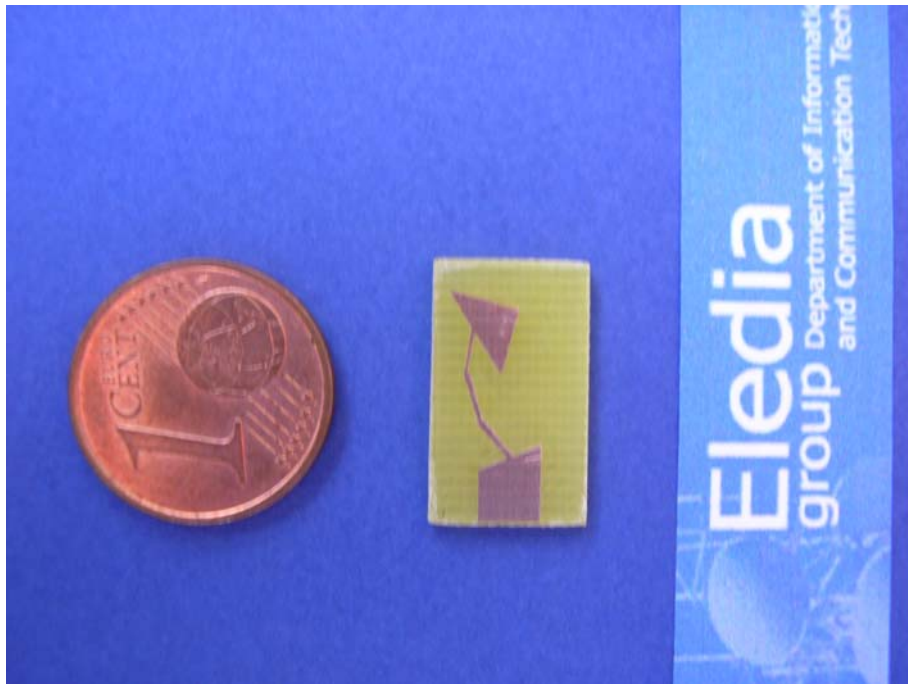


Fig. 4 – R.Azaro et al. “Design of a pre-fractal monopolar antenna”

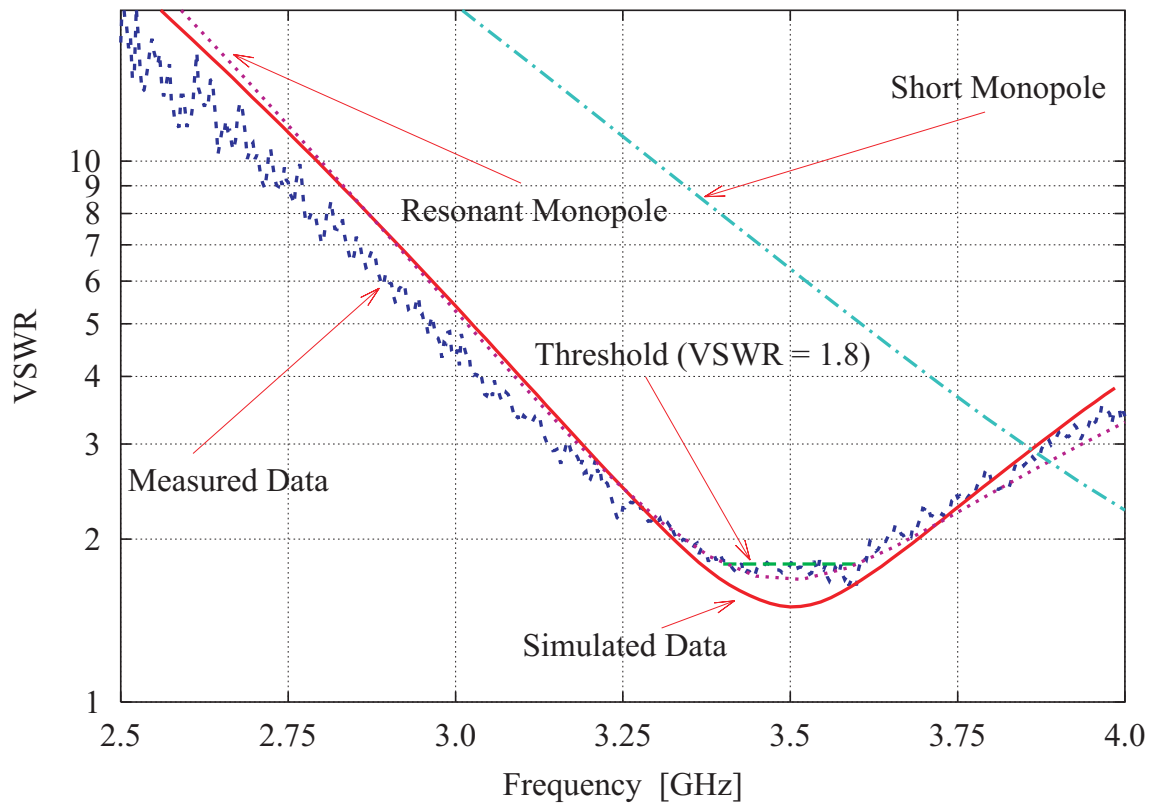
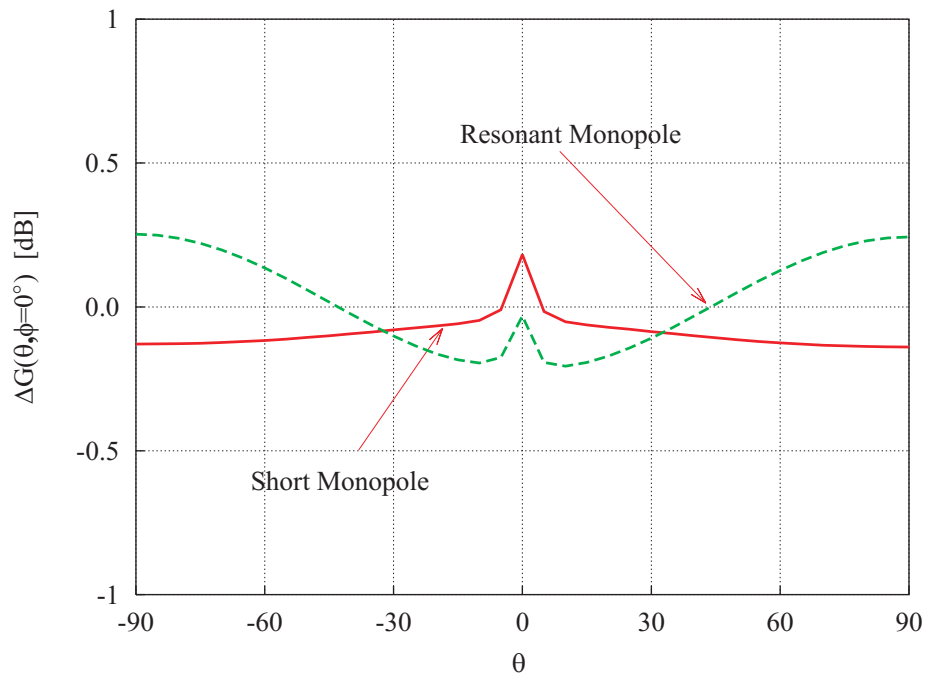
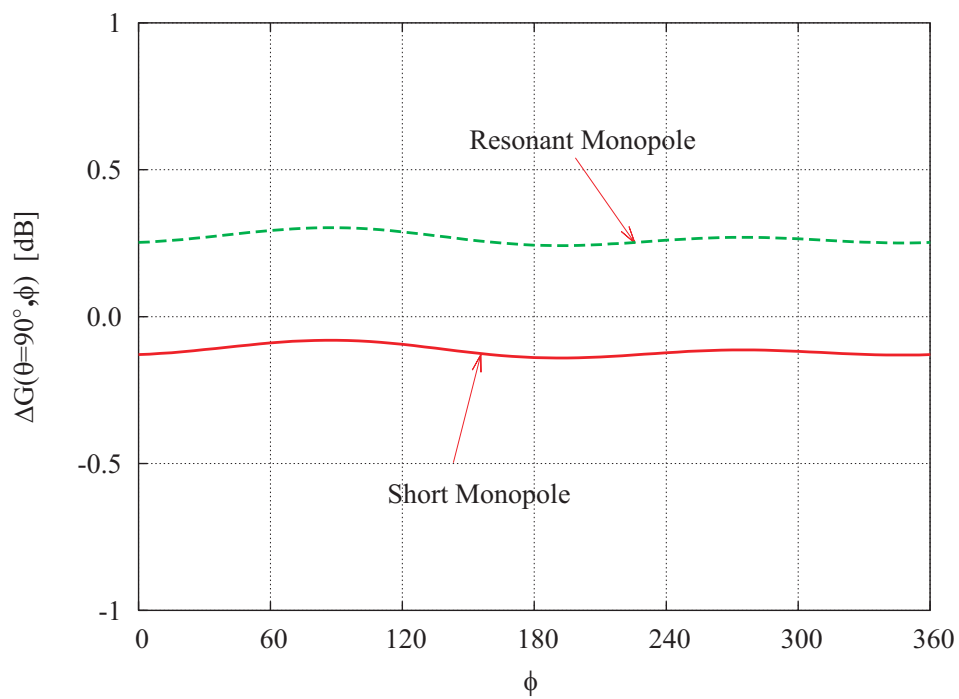


Fig. 5 – R.Azaro *et al.*, “Design of a pre-fractal monopolar antenna”



(a)



(b)

Fig. 6 – R.Azaro et al., “Design of a pre-fractal monopolar antenna ...”